Nuclear Instruments and Methods in Physics Research A 816 (2016) 160–170

Contents lists available at ScienceDirect

Nuclear Instruments and Methods in Physics Research A

journal homepage: www.elsevier.com/locate/nima

Measurement of longitudinal electron diffusion in liquid argon

Yichen Li [a,*], Thomas Tsang [b], Craig Thorn [a], Xin Qian [a], Milind Diwan [a], Jyoti Joshi [a], Steve Kettell [a], William Morse [a], Triveni Rao [b], James Stewart [a], Wei Tang [a], Brett Viren [a]

[a] Physics Department, Brookhaven National Laboratory, 20 Pennsylvania St., Building 510E, Upton, NY 11973, USA
[b] Instrumentation Division, Brookhaven National Laboratory, 20 N. Technology St., Building 535B, Upton, NY 11973, USA

ARTICLE INFO

Article history:
Received 27 August 2015
Received in revised form
25 January 2016
Accepted 29 January 2016
Available online 7 February 2016

Keywords:
Liquid argon time projection chamber
Electron diffusion
Electron drift velocity
Photocathode
Longitudinal diffusion
Electron mobility

ABSTRACT

We report the measurement of longitudinal electron diffusion coefficients in liquid argon for electric fields between 100 and 2000 V/cm with a gold photocathode as a bright electron source. The measurement principle, apparatus, and data analysis are described. In the region between 100 and 350 V/cm, our results show a discrepancy with the previous measurement [1]. In the region between 350 and 2000 V/cm, our results represent the world's best measurement. Over the entire measured electric field range, our results are systematically higher than the calculation of Atrazhev-Timoshkin [2]. The quantum efficiency of the gold photocathode, the drift velocity and longitudinal diffusion coefficients in gas argon are also presented.

1. Introduction

The development of the liquid argon (LAr) ionization chamber pioneered by Willis and Radeka [3] was an important advance in high energy calorimetry, and was quickly followed by the development of the LAr time projection chamber (TPC) [4] as a fine-grained tracking calorimeter for high energy physics experiments. LArTPCs are now the preferred technology for many accelerator neutrino and dark matter experiments. At present, two LArTPCs have been constructed and operated for neutrino physics measurements: the ICARUS [5] detector in Italy and the ArgoNeut [6] detector in the US. Meanwhile, two other LArTPCs have been constructed for dark matter searches: Darkside [7] and WArP [8] detectors. In the near term the MicroBooNE experiment, with a 170 ton LArTPC, has begun operation in the US [9]. In the future, a set of LArTPCs will be installed at Sanford Underground Research Facility (SURF) for the Deep Underground Neutrino Experiment (DUNE) to search for CP violation in the lepton sector and to determine the neutrino mass hierarchy [10]. For the near-term neutrino program [11], a three-LArTPC configuration [12] will be implemented at Fermilab to search for a light sterile neutrino and to precisely measure neutrino-argon interaction cross sections.

LArTPCs are attractive detectors for neutrino experiments. As the most abundant noble gas ($\sim 1.3\%$ by weight) in the atmosphere, argon is commercially available in large quantities. The low cost and relative high density (~ 1.4 g/ml at 87 K) make LAr an ideal material for the massive TPCs needed for neutrino-induced rare processes. Their resulting charged particles transverse through the LAr and produce ionization electrons and scintillation light. Electrons in the ionization track will then drift at constant velocity along the lines of an applied electric field. The coordinate information perpendicular to the electron drift direction can be determined with a high-resolution, two-dimensional charge detector (e.g. wire planes). The scintillation light provides a fast indication of initial activity. By measuring the time delay to the subsequent signal from the drifting charge, it is possible to determine the distance over which the electrons drifted. The spatial resolution of the interaction point and the detailed topology of the subsequent particle trajectories can reach the millimeter level. The reconstructed event topology can be used for the particle identification and, along with measuring the total amount of drifted charge, it can be used to determine the energy deposited in the detector. The charge collected per wire per unit time is closely related to the energy deposition per unit distance (dE/dx), which can also be used for the particle identification and the energy reconstruction. Therefore, the excellent signal efficiency and background rejection that result from these characteristics make LArTPCs ideal for neutrino experiments.

In order to fully optimize the extraction of the intrinsic physics information from the recorded charge signal and to properly simulate the performance of LArTPCs, knowledge of the transport properties of electrons in LAr is essential. In particular, the diffusion of electrons drifting in the electric field from the point of ionization to the anode read-out plane is an important quantity contributing to the ultimate spatial resolution of the future long-drift-distance (up to 20 m)

* Corresponding author. Tel.: +1 631 344 7405; fax: +1 631 344 4741.
E-mail address: yichen@bnl.gov (Y. Li).

http://dx.doi.org/10.1016/j.nima.2016.01.094
0168-9002/

detectors. The diffusion of electrons in strong electric fields is generally not isotropic. Therefore, longitudinal and transverse diffusion require separate measurements. For most substances the diffusion in the direction of the drift field (longitudinal diffusion) is smaller than the diffusion in the direction transverse to the field (transverse diffusion). Measurements have been reported previously of transverse diffusion at electric fields above 1500 V/cm [13,14] and for longitudinal diffusion between 100 and 350 V/cm [1]. In this paper we report a complete set of measurements of the longitudinal diffusion coefficient for electrons drifting in LAr at fields from 100 and 2000 V/cm. In Section 2, we review the basic formalism of electron diffusion in LAr. In Section 3, we describe our experimental apparatus. In Section 4, we describe the procedure of data taking and the analysis of the raw waveforms. In Section 5, we discuss the systematic uncertainties in our measurement. In Section 6, we report the results of electron drift velocity and diffusion in liquid argon as well as gas argon. A summary is presented in Section 7.

2. Electron diffusion in liquid argon

When a macroscopic swarm of electrons moves through a medium under the influence of an electric field, three processes are necessary to adequately describe its time development. They are (1) the drift velocity of the swarm centroid, (2) the diffusional growth of the volume of the swarm, and (3) the loss or gain of electrons in the swarm due to attachment to atoms or molecules in the medium or to ionization of the medium. In liquid argon at the fields considered here, ionization does not occur. The differential equation describing the time evolution of the electron density in the swarm is expressed by (Fick's equation [15,16]):

$$\frac{\partial n}{\partial t} = D_L\frac{\partial^2 n}{\partial z^2} + D_T\left(\frac{\partial^2 n}{\partial x^2} + \frac{\partial^2 n}{\partial y^2}\right) - v\frac{\partial n}{\partial z} - \lambda v n \tag{1}$$

where $n \equiv n(x,y,z,t)$ is the electron charge density distribution at position (x,y,z) and time t. The drift occurs with velocity v in the z (longitudinal) direction as shown in Fig. 1. v is the drift velocity. D_L and D_T are the longitudinal and transverse diffusion coefficients, respectively. The attachment coefficient minus the ionization coefficient is represented by λ. Since ionization does not contribute in our case, the inverse of λ is equal to the mean free path. The solution to this equation for an initial point source of charge at the origin with a constant field in the z direction is described by a distribution function

$$n(\rho,z,t) = \frac{n_0}{4\pi D_T t\sqrt{4\pi D_L t}}\exp\left(-\frac{(z-vt)^2}{4D_L t} - \lambda v t\right)\exp\left(-\frac{\rho^2}{4D_T t}\right) \tag{2}$$

where $\rho^2 = x^2 + y^2$ is the transverse coordinate. This distribution is a Gaussian function of z and ρ at an instant in time, but is not a Gaussian in time at a fixed point in space. The electron current measured on a plane perpendicular to the drift direction at a distance d from the point source (i.e. the anode) is

$$j(t) = 2\pi\int \rho\cdot n(\rho,d,t)\cdot d\rho = \frac{n_0}{\sqrt{4\pi D_L t}}\exp\left(-\frac{(d-vt)^2}{4D_L t} - \lambda v t\right). \tag{3}$$

This function approaches a Gaussian distribution for large $d\cdot v$ and small D_L, which is a reasonable approximation for our study. For this signal, the time at the peak, t_p, is given by:

$$t_p = \frac{-D_L + \sqrt{D_L^2 + d^2 v(v+4D_L\lambda)}}{v(v+4D_L\lambda)} \tag{4}$$

where d is the drift distance. The measured drift velocity v_M is defined as the drift distance d divided by the time at the peak t_p. The longitudinal diffusion width in time σ_L, defined as the standard deviation in time of this charge distribution, can be similarly

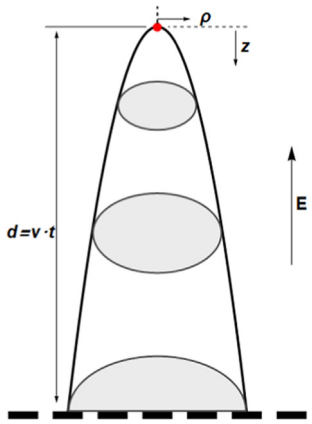

Fig. 1. Illustration of the diffusion process starting from a point source to the detection plane indicated by dashed line. The diffusion in the longitudinal direction (along the drift direction) is generally expected to be smaller than that of the transverse direction. The standard deviation of the electron swarm (indicated by the shaded ellipses in the figure at three drift times) is expected to follow Eq. (9).

computed in terms of the true drift velocity v, the diffusion coefficient D_L, and the attachment coefficient λ. The resulting expression is

$$\sigma_L^2 = \frac{2\left(d^2v_c^2 - 3D_L(-3D_L + \sqrt{D_L^2 + d^2v_c^2}) - dv_c(-4D_L + \sqrt{D_L^2 + d^2v_c^2})\right)}{v_c^4} \tag{5}$$

with $v_c = \sqrt{v(v+4D_L\lambda)}$. For the longitudinal standard deviation we use the term diffusion time.

The expression for the measured velocity and the diffusion time can be expanded in a power series in D_L to display the dependence on the parameters. The results of expanding both v_M and σ_L in powers of D_L are

$$v_M = v\left(1 + \frac{D_L}{dv} + \frac{D_L^2}{2d^2v^2} + \frac{2D_L\lambda}{v} - \frac{2D_L^2\lambda^2}{v^2} + O(D_L^3,\lambda^3)\right)$$

$$\sigma_L^2 = \frac{2dD_L}{v^3}\left(1 + \frac{17D_L}{2dv} - \frac{3D_L^2}{2d^2v^2} - \frac{6D_L\lambda}{v} - \frac{68D_L^2\lambda}{dv^2} + \frac{30D^2\lambda^2}{v^2} + O(D_L^3,\lambda^3)\right).$$

Provided that the dimensionless variables $\alpha = D_L/(dv) \ll 1$ and $\beta = \alpha d\lambda \ll 1$, the values of v_M and σ_L^2 are well approximated by the first (zero order) terms in the expansions. Note that for attachment coefficients as large as $\lambda = 1/d$, the condition that $\beta \ll 1$ is still satisfied. The full expression for v_M can be inverted to give v in terms of v_M, D_L and λ, but the expression for σ_L^2 cannot be inverted. However, by substituting the expression for v into the second series above, and applying Lagrange reversion [17] to the result, we can obtain the series expansions for the true quantities in terms of the measured ones. To simplify the result, we define the measured diffusion coefficient as

$$D_{L,M} = \frac{v_M^3\sigma_L^2}{2d}. \tag{6}$$

In terms of the directly measured quantities with $v_M = d/t_p$, it is

$$D_{L,M} = \frac{d^2\sigma_L^2}{2t_p^3}. \tag{7}$$

With this definition, the two inverted series can be expressed in terms of the small dimensionless variables $\alpha_M = D_{L,M}/(dv_M)$ and $\beta_M = \alpha_M d\lambda$ as:

$$v = v_M\left(1 - \alpha_M + 11\alpha_M^2 - \tfrac{427}{2}\alpha_M^3 - 2\beta_M + 23\alpha_M\beta_M + 2\beta_M^2 - 449\alpha_M^2\beta_M - 44\alpha\beta^2 + O(\alpha_M^4,\beta_M^3)\right),$$